Nitric oxide synthase 2 is required for conversion of pro-fibrogenic inflammatory CD133+ progenitors into F4/80+ macrophages in experimental autoimmune myocarditis

Blyszczuk, Przemyslaw ; Berthonneche, Corrine ; Behnke, Silvia ; Glönkler, Marcel ; Moch, Holger ; Pedrazzini, Thierry ; Lüscher, Thomas F ; Eriksson, Urs ; Kania, Gabriela

Abstract: AIMS: Experimental Autoimmune Myocarditis (EAM) model mirrors important mechanisms of inflammatory dilated cardiomyopathy (iDCM). In EAM, inflammatory CD133(+) progenitors are a major cellular source of cardiac myofibroblasts in post-inflammatory myocardium. We hypothesized that exogenous delivery of Macrophage-Colony Stimulating Factor (M-CSF) can stimulate macrophage lineage differentiation of inflammatory progenitors and therefore prevent their naturally occurring myofibroblast fate in EAM.Methods and ResultsEAM was induced in wild-type (BALB/c) and Nitric oxide synthase 2 deficient (Nos2(-/-)) mice and CD133(+) progenitors were isolated from inflamed hearts. In vitro, M-CSF converted inflammatory CD133(+) progenitors into nitric oxide-producing F4/80(+) macrophages and prevented TGF- -mediated myofibroblast differentiation. Importantly, only a subset of heart-infiltrating CD133(+) progenitors expresses macrophage-specific antigen F4/80 in EAM. These CD133(+)/F4/80(hi) cells show impaired myofibrogenic potential compared to CD133(+)/F4/80(-) cells. M-CSF treatment of wild-type mice with EAM at the peak of disease markedly increased CD133(+)/F4/80(hi) cells in the myocardium, and CD133(+) progenitors isolated from M-CSF-treated mice failed to differentiate into myofibroblasts. In contrast, M-CSF was not effective in converting CD133(+) progenitors from inflamed hearts of Nos2(-/-) mice into macrophages, and M-CSF treatment did not result in increased CD133(+)/F4/80(hi) cell population in hearts of Nos2(-/-) mice. Accordingly, M-CSF prevented post-inflammatory fibrosis and left ventricular dysfunction in wild-type but not in Nos2(-/-) mice. CONCLUSIONS: Active and NOS2-dependent induction of macrophage lineage differentiation abrogates the myofibrogenic potential of heart-infiltrating CD133(+) progenitors. Modulating the in vivo differentiation fate of specific progenitors might become a novel approach for the treatment of inflammatory heart diseases.

DOI: https://doi.org/10.1093/cvr/cvs317

DOI: https://doi.org/10.1093/cvr/cvs317

Cardiovascular Research Advance Access published October 22, 2012

Nitric oxide synthase 2 is required for conversion of pro-fibrogenic inflammatory CD133$^+$ progenitors into F4/80$^+$ macrophages in experimental autoimmune myocarditis

Przemyslaw Blyszczuk[1,2], Corrine Berthonneche[3], Silvia Behnke[4], Marcel Glönkler[5], Holger Moch[5], Thierry Pedrazzini[3], Thomas F. Lüscher[1,6], Urs Eriksson[1,2#], Gabriela Kania[1,2#]

[1]Cardiovascular Research and Zürich Center for Integrative Human Physiology; Institute of Physiology, University of Zürich, Winterthurerstr. 190, CH-8057 Zürich, Switzerland; [2]Department of Medicine, GZO - Zürich Regional Health Center, Spitalstr. 66, CH-8620 Wetzikon, Switzerland; [3]Experimental Cardiology Unit, Department of Medicine, University of Lausanne Medical School, CH-1011 Lausanne, Switzerland [4]Sophistolab AG, Bauelenzelgstrasse 20, 8193 Eglisau, Switzerland, [5]Institute for Surgical Pathology, Department of Pathology; [6]Department of Cardiology; University of Zurich, Switzerland; Winterthurerstr. 190, CH-8057 Zürich, and University Hospital Zürich, Rämistr. 100, CH-8001 Zürich, Switzerland

Corresponding author:

Gabriela Kania, PhD

Cardioimmunology, Cardiovascular Research, Institute of Physiology, University of Zürich

Winterthurerstrasse 190, CH-8057 Zürich, Switzerland

phone: ++41-44-6354995; fax: ++41-44-2558701

E-mail: gabriela.kania@uzh.ch

[#] Shared last authorship

Abstract

Aims: Experimental Autoimmune Myocarditis (EAM) model mirrors important mechanisms of inflammatory dilated cardiomyopathy (iDCM). In EAM, inflammatory $CD133^+$ progenitors are a major cellular source of cardiac myofibroblasts in post-inflammatory myocardium. We hypothesized that exogenous delivery of Macrophage-Colony Stimulating Factor (M-CSF) can stimulate macrophage lineage differentiation of inflammatory progenitors and therefore prevent their naturally occurring myofibroblast fate in EAM.

Methods and Results: EAM was induced in wild-type (BALB/c) and Nitric oxide synthase 2 deficient (*Nos2*$^{-/-}$) mice and $CD133^+$ progenitors were isolated from inflamed hearts. *In vitro,* M-CSF converted inflammatory $CD133^+$ progenitors into nitric oxide-producing $F4/80^+$ macrophages and prevented TGF-β-mediated myofibroblast differentiation. Importantly, only a subset of heart-infiltrating $CD133^+$ progenitors expresses macrophage-specific antigen F4/80 in EAM. These $CD133^+/F4/80^{hi}$ cells show impaired myofibrogenic potential compared to $CD133^+/F4/80^-$ cells. M-CSF treatment of wild-type mice with EAM at the peak of disease markedly increased $CD133^+/F4/80^{hi}$ cells in the myocardium, and $CD133^+$ progenitors isolated from M-CSF-treated mice failed to differentiate into myofibroblasts. In contrast, M-CSF was not effective in converting $CD133^+$ progenitors from inflamed hearts of *Nos2*$^{-/-}$ mice into macrophages, and M-CSF treatment did not result in increased $CD133^+/F4/80^{hi}$ cell population in hearts of *Nos2*$^{-/-}$ mice. Accordingly, M-CSF prevented post-inflammatory fibrosis and left ventricular dysfunction in wild-type but not in *Nos2*$^{-/-}$ mice.

Conclusions: Active and NOS2-dependent induction of macrophage lineage differentiation abrogates the myofibrogenic potential of heart-infiltrating $CD133^+$ progenitors. Modulating the *in vivo* differentiation fate of specific progenitors might become a novel approach for the treatment of inflammatory heart diseases.

Key words: experimental autoimmune myocarditis, CD133 progenitor, M-CSF, myofibroblast, macrophage**,** nitric oxide synthase 2

Introduction

Inflammatory dilated cardiomyopathy (iDCM) is an important cause of heart failure and sudden death in children and young patients[1]. Progressive cardiac dilation and fibrosis are hallmarks of iDCM in humans. iDCM refers to an end stage heart failure phenotype which often results from virus-triggered myocarditis[2]. Both, clinical observations and animal experiments suggest that infection-triggered autoimmunity plays an important role in iDCM[3]. Heart-specific autoimmune responses are a consequence of the lack of T cell tolerance to heart-specific alpha-myosin heavy chain (αMyHC) in mice and in humans[4].

Experimental autoimmune myocarditis (EAM) is a $CD4^+$ T cell-mediated mouse model of iDCM. In susceptible mouse strains, EAM is commonly induced after immunization with αMyHC peptide together with a strong adjuvant[4]. In BALB/c mice, the extent of cardiac infiltrates peaks three weeks after immunization. Inflammatory infiltrates largely resolve thereafter, but the process of pathological remodelling continues and many mice develop an end stage heart failure phenotype, including ventricular dilation, myocardial fibrosis and heart failure on follow-up[5].

At the peak of EAM, inflammatory cells, including granulocytes, monocytes, macrophages, T cells, B cells, and $CD133^+$ progenitors infiltrate the myocardium[4, 6]. CD133 (prominin-1) and its human orthologue, AC133, are often expressed on primitive cell populations including hematopoietic stem cells. In EAM, bone marrow-derived $CD133^+$ progenitors represent the major cellular source of collagen-producing fibroblasts involved in the progressive Transforming Growth Factor-beta (TGF-β)-mediated cardiac remodelling[6], which reflects the transition from acute inflammation into the typical end stage heart failure phenotype.

Macrophages represent another important heart-infiltrating cell subset in EAM[7]. In mice, macrophages commonly express the F4/80 antigen. Their role in disease pathogenesis, however, remains controversial. So far, the nitric oxide synthase 2 (NOS2)-expressing M1 macrophage subset had been considered to contribute to disease progression[7, 8], On the other hand, nitric oxide also acts as a strong immunosuppressive molecule preventing EAM development via induction of T cell apoptosis[6]. Alternatively activated M2 macrophages, are considered to promote resolution of inflammation and reduce disease severity[7-9].

Macrophage-colony stimulating factor (M-CSF) is one of the key cytokines regulating immune responses and reparative processes in many inflammatory and cardiovascular disorders[10, 11]. M-CSF plays a pivotal role in differentiation and maturation of the macrophage myeloid lineage[12]. Mice lacking functional M-CSF show macrophage deficiency, reduced phagocytosis and strongly impaired nitric oxide production[13]. In animal models of ischemic heart failure and viral myocarditis, M-CSF treatment improves cardiac function[14, 15,16], but the mechanism is still unclear.

We hypothesize that altering the *in vivo* fate of inflammatory progenitors by selectively promoting macrophage lineage differentiation, may protect from myofibroblast accumulation and cardiac fibrosis in EAM. In fact, M-CSF induced conversion of heart-infiltrating $CD133^+$ progenitors into $F4/80^+$ macrophages and prevented their myofibroblast differentiation in the post-inflammatory phase of EAM. Moreover, our data points to critical role of NOS2 and nitric oxide in M-CSF-dependent macrophage lineage differentiation of inflammatory $CD133^+$ progenitors. Thus, we demonstrate how exogenous cytokine treatments may change the default differentiation fate of inflammatory progenitors and can prevent pathological tissue remodelling in iDCM.

Methods

Mice

BALB/c (n=250) and *Nos2*$^{-/-}$ (n=50) mice on BALB/c background were used in this study. Animal experiments were performed in accordance with the Swiss federal law and with the Guide for the Care and Use of Laboratory Animals published by the US National Institutes of Health (NIH Publication, 8th Edition, 2011). All animal experiments were approved by the Cantonal Veterinary Office in Zürich.

EAM induction and cytokine treatments

Mice were injected subcutaneously with 150 µg of αMyHC (Ac-RSLKLMATLFSTYASADR-OH; Caslo) peptide emulsified 1:1 with Complete Freund's Adjuvant (CFA, Difco) on days 0 and 7. 200 µg/kg M-CSF (Peprotech) were intravenously injected 5x every second day between days 21-29 or days 40-48 of EAM. Control mice received solvent only.

Histopathology and Immunocytochemistry

Hearts were formalin-fixed and paraffin-embedded. Heart sections were stained with rat anti-mouse CD45 (BD Bioscience), rabbit anti-mouse CD3 (Neomarkers), rat anti-mouse F4/80 (BMA biomedicals) and rabbit anti-rat IgG (Abcam) antibodies, and with Bond Polymer Refine Detection kit using BOND-MAX system (both Leica). Masson's Trichrom staining was used to detect fibrosis. Immunopositive cells and fibrotic areas were quantified using analySIS FIVE software (Olympus).

Echocardiography

Mice were lightly anesthetized with 1-1.5% isoflurane, maintaining heart rate at 400-500 beats per minute. Transthoracic echocardiography was performed using a 30 MHz probe and the Vevo 770 Ultrasound system (VisualSonics) as described[17] and in Supplementary Material.

Cell cultures

Myocarditis-positive hearts were perfused, dissected and digested with Liberase Blendzyme (Roche) for 45

min at 37˚C and tissue suspensions were passed sequentially through 70 µm and 40 µm cell strainers. Cardiomyocytes were separated by low speed centrifugation (50 g, 2 min). $CD133^+$ cells were isolated by positive selection using anti-CD133-PE antibody (eBioscience) and magnetic anti-PE-microbeads (Miltenyi) or using FACS. Enriched $CD133^+$ cells were plated onto gelatine-coated cell culture plates and cultured in the Iscove's Modified Dulbecco's Medium supplemented with 20% foetal bovine serum, 1:100 penicillin/streptomycin, 100 mM non-essential amino acids, 100 mM sodium pyruvate and 50mM β-mercaptoethanol (all Invitrogen). Macrophage differentiation was induced with 10 ng/mL M-CSF, and fibroblast differentiation with 10 ng/mL TGF-β (both PeproTech).

Flow cytometry and cell sorting

Single cell suspensions were prepared from digested hearts and cultured cells. Cells were incubated 30 min on ice with the appropriate combination of fluorochrome- or biotin-conjugated antibodies. The following antibodies were used: anti-CD45-FITC, anti-CD45-PE, anti-NOS2-FITC (all BD Bioscience), anti-CD133-PE, anti-F4/80-PE (both eBioscience), biotin-conjugated anti-F4/80 (Cedarlane), anti-CD16/32 (Miltenyi), anti-CD206 (Biolegend), anti-CD301 (Serotec), anti-CD133 (eBioscience). Streptavidin-APC (BD Bioscience) was used to detect biotin-conjugated antibodies. Cells were analysed with the FACSCanto analyser (BD Bioscience) and FlowJo software (Tree Star). In some experiments, cells were sorted with FACSAria III (BD Bioscience).

Quantitative RT-PCR

Total RNA was isolated using RNeasy micro kit (Qiagen). cDNAs were amplified using the Power SYBR Green PCR Master Mix (Applied Biosystems) and oligonucleotides complementary to transcripts of the analyzed genes using the 7500 Fast Real-Time PCR System (Applied Biosystems). The following oligonucleotides were used in this study: αSMA (*Acta2*): 5'-cgctgtcaggaaccctgaga-3', 5'-cgaagccggccttacaga-3'; collagen I (*Col1a1*): 5'-gatgacgtgcaatgcaatgaa-3', 5'-ccctcgactcctacatcttctga-3'; fibronectin (*Fn1*): 5'-taccaaggtcaatccacacccc-3', 5'-cagatggcaaaagaaagcagagg-3'; gapdh (*Gapdh*): 5'-ctgcaccaccaactgcttagc-3', 5'-ggcatggactgtggtcatgag-3'. Transcript levels of gapdh were used as endogenous reference, and relative gene expression was analyzed using the $2^{-\Delta\Delta Ct}$ method.

Immunohistochemistry and phagocytosis assays

Cells were cultured on gelatine-coated cover slips and fixed with 4% paraformaldehyde or methanol:acetone (7:3). 1% bovine serum albumin was used as blocking solution. The following antibodies were used: mouse IgG anti-αSMA (Sigma), rabbit IgG anti-fibronectin (Milipore), AlexaFluor488 anti-mouse IgG and AlexaFluor546 anti-rabbit IgG 1:600 (both Invitrogen). DAPI was used to label nuclei. Alexa Fluor 488-conjugated Escherichia coli BioParticles (Invitrogen) were used according to manufacturer's recommendations. Immunofluorescence was analysed using the Olympus BX51 fluorescence microscope.

Statistics

Normally distributed data were analysed by unpaired, two-tailed Student's *t*-test and by one-way ANOVA followed by Bonferroni post-hoc test. Severity scores were analysed by the one-way Kruskal-Wallis analysis. For correlation analysis, Pearson's correlation coefficient was calculated. All analyses were computed using GraphPad Prism 5 software. Differences were considered as statistically significant for $p<0.05$.

Results

M-CSF converts heart-infiltrating CD133$^+$ progenitors into functional F4/80$^+$ macrophages, and prevents TGF-β-induced myofibroblast differentiation *in vitro*.

BALB/c mice receiving two subcutaneous injections of αMyHC/CFA at days 0 and 7 develop severe myocarditis at day 21. At this stage, CD133$^+$ progenitors represent about 30% of all CD45$^+$ inflammatory cells in the heart[6]. To assess the differentiation capacity of these cells at the peak of disease, CD133$^+$ cells were isolated from diseased hearts at day 21 of EAM, plated and expanded for two weeks *in vitro*. Expanded cells were cultured in the presence or absence of M-CSF or TGF-β for additional 14 days. In the presence of TGF-β, CD133$^+$ cells differentiated into myofibroblasts, positive for αSMA and fibronectin (Fig. 1A-B). In contrast, addition of M-CSF failed to trigger myofibroblast differentiation (Fig. 1A-B) and pre-treatment of CD133$^+$ cells with M-CSF for 3 days prevented TGF-β-triggered myofibroblast formation (Fig. 1C-D).

In cytokine-free cultures, most expanded cells remained positive for CD133 and were mainly negative for macrophage marker F4/80 (Supplementary Figure 1A-B). In the presence of M-CSF, however, CD133 expression was reduced (Supplementary Figure 1A) and cells up-regulated F4/80, CD11b and CD16/32, suggesting macrophage lineage differentiation (Supplementary Figure 1B-D). Cells cultured with M-CSF developed into fully active macrophages producing NOS2, secreting nitric oxide and phagocyting *E.coli* bacteria (Supplementary Figure 1E,F,J). Of note, M-CSF treatment did not affect expression of markers characteristic for alternatively activated M2 macrophages (CD206, CD301, Supplementary Figure 1G-H) or markers characteristic for granulocytes or dendritic cells, i.e. Gr-1 (Ly6C, Supplementary Figure 1I), MHC class II and CD11c (not shown).

To address the immunomodulating potential of CD133$^+$ progenitors and CD133$^+$-derived M-CSF-differentiated macrophages we co-cultured them with αMyHC-reactive Th17 cell lines in the presence of αMyHC-pulsed irradiated splenocytes as antigen presenting cells. On irradiated splenocytes, αMyHC-reactive CD4$^+$ T cells proliferated rapidly. In the presence of CD133$^+$ progenitors or M-CSF-differentiated macrophages, however, proliferation was completely abolished (Supplementary Figure 2A). Further, we induced EAM in BALB/c mice and additionally administrated intravenously 2x10^6 of either *in vitro*

expanded CD133$^+$ progenitors or CD133$^+$-derived mature macrophages at day 7 after EAM induction and analysed myocarditis severity at day 21. In animals treated with both, CD133$^+$ progenitors and M-CSF-differentiated macrophages practically no myocarditis was observed compared to sham treated mice (Supplementary Figure 2B). In contrast, administration of M-CSF-differentiated macrophages expanded from *Nos2*$^{-/-}$ mice failed to protect from myocarditis (Supplementary Figure 2C). These latter findings confirm the protective and NOS2-dependent role of CD133$^+$-derived M-CSF-differentiated macrophages in EAM.

M-CSF treatment promotes accumulation of F4/80$^+$ macrophages in the post-inflammatory heart

At day 21, inflamed hearts contained a substantial pool of CD133$^+$ progenitors, but fibrosis was not evident at this time point. As illustrated above, M-CSF effectively directs CD133$^+$ progenitors into functional macrophages and prevents their myofibroblast differentiation. We therefore analysed how systemic M-CSF treatment of αMyHC/CFA-immunized mice affects the pattern of heart-infiltrating cell subsets. Accordingly, αMyHC/CFA-immunized mice received M-CSF injections between days 21-29 of EAM (Supplementary figure 3A). Three days after the first M-CSF injection, we observed significantly increased number of F4/80$^+$ and CD133$^+$ cells in the myocardium of M-CSF treated mice (day 24, Figure 2A-B). Immunopositive F4/80$^+$ macrophages in the myocardium decreased over time and remained at low numbers at day 40 (Figure 2A; Supplementary Figure 4A-B). M-CSF treatments, however, did not affect the expression of CD16/32, CD206 and CD301 in inflammatory macrophages (Figure 2E-G). Instead, we observed significantly increased NOS2 on F4/80$^+$ cells in the heart after M-CSF treatment of wild-type mice (Figure 2D).

M-CSF inhibits formation of myofibroblasts from inflammatory CD133$^+$ progenitors in EAM

Heart-infiltrating CD133$^+$ progenitors represent the major cellular source of myofibroblasts in post-inflammatory EAM[6]. At day 24 of EAM, we sorted inflammatory (CD45-positive) CD133$^+$/F4/80$^-$ and CD133$^+$/F4/80^{hi} cells from the inflamed myocardium of BALB/c mice and found elevated levels of myofibroblast-specific genes in CD133$^+$ cells negative for F4/80 (Figure 3A-B). These findings suggest that CD133$^+$/F4/80$^-$ rather than CD133$^+$/F4/80^{hi} cells contribute to fibrogenesis in post-inflammatory EAM.

M-CSF-stimulated CD133$^+$ progenitors acquired a functional macrophage phenotype within 3 days i*n vitro* (Figure 2H). We therefore analysed F4/80 expression on heart-infiltrating CD133$^+$ progenitors in M-CSF-treated mice. We found that heart-infiltrating CD133$^+$/CD45$^+$ cells of M-CSF-treated mice had marked higher F4/80 at day 24 (i.e. 3 days after the cytokine treatment, Figure 3C-D). Next, we sorted heart-infiltrating CD133$^+$/CD45$^+$ cells from PBS- and M-CSF-treated mice and found reduced mRNA levels of myofibroblast-specific genes in the M-CSF-treated group (Figure 3E). Furthermore, sorted heart-infiltrating CD133$^+$/CD45$^+$ cells from both groups were plated and cultured in the presence of TGF-β for 10 days. CD133$^+$/CD45$^+$ cells isolated from the myocardium of M-CSF-treated mice failed to differentiate into αSMA- and fibronectin-expressing myofibroblasts (Figure 3F).

NOS2 controls M-CSF-dependent macrophage differentiation of heart-infiltrating CD133$^+$ progenitors

F4/80^{hi} macrophages derived from CD133$^+$ progenitors up-regulate NOS2 and produce nitric oxide. We therefore addressed the role of NOS2 in the macrophage differentiation processes. Accordingly, CD133$^+$ progenitors were isolated at day 21 after immunization from inflamed hearts of wild-type or *Nos2*$^{-/-}$ mice and cultivated in the presence of M-CSF. *Nos2*$^{-/-}$ CD133$^+$ progenitors showed reduced F4/80 and CD14 expression and were functionally impaired as indicated by reduced *E.coli* phagocytosis (Figure 4A-E). To determine whether macrophage differentiation was mediated by NOS activity, CD133$^+$ progenitors isolated from inflamed hearts of BALB/c mice were cultured for 3 days in the presence of M-CSF with or without L-NAME, a non-specific NOS inhibitor. Cells cultured with L-NAME showed significantly reduced *E.coli* phagocytosis (Figure 4F) and reduced nitric oxide levels (Figure 4G).

M-CSF treatment prevents cardiac fibrosis and left ventricular dysfunction in EAM

M-CSF prevents TGF-β-mediated myofibroblast differentiation and promotes formation of macrophages from inflammatory CD133$^+$ progenitors. Given that CD133$^+$ progenitors represent the major source for myofibroblasts in EAM, we addressed whether M-CSF treatment reduces fibrogenesis in the post-inflammatory heart. Accordingly, we treated αMyHC/CFA-immunized mice with M-CSF between days 21-29 or 40-48 of EAM, and analysed the hearts at day 40 and 60 respectively (Supplementary figure 3A). As

illustrated in the Figure 5, M-CSF treatment completely prevented accumulation of fibroblasts in the post-inflammatory heart (Figure 5A-C; Supplementary figure 4B). Of note, M-CSF treatment failed to attenuate fibrosis when delivered between days 40-48 (Figure 5A). These findings suggest that M-CSF treatment prevented the fibrotic process, but did not revert already established cardiac fibrosis.

Relapses of inflammatory cells are quite common in autoimmune diseases. In BALB/c mice, we observed spontaneous inflammatory relapses 40 days after the first immunization (Figure 5D-E). During relapses, $CD45^+$ inflammatory cells were mainly detected in the pericardium and largely represented $CD3^+$ T lymphocytes (Figure 5D-E, Supplementary figure 3C). Interestingly, M-CSF treatment between days 21-29 inhibited relapses in αMyHC/CFA-immunized mice as reflected by reduced numbers of $CD45^+$ and $CD3^+$ T cells in the myocardium at day 40 (Figure 5D-E; Supplementary figure 3C).

Cardiac fibrosis parallels both, diastolic dysfunction, and reduced cardiac contractility. Not all immunized mice develop severe myocarditis. Consequently the extent of post-inflammatory fibrosis varies in the EAM model. In our series, 11 out of 20 αMyHC/CFA-immunized BALB/c mice showed substantial fibrosis (>2% of total heart area) on day 40. At this time point, echocardiography revealed reduced ejection fraction and fractional shortening in mice with significant fibrosis (Figure 5F). In addition, the extent of fibrosis correlated with increased mass, systolic and diastolic volume and isovolumetric contraction time of the left ventricle (Supplementary Figure 5A). Echocardiography of αMyHC/CFA-immunized and M-CSF-treated mice showed unaffected cardiac function at day 40 (Figure 5F, Supplementary Figure 5E).

Next, we immunized *Nos2*$^{-/-}$ mice with αMyHC/CFA and treated with M-CSF or PBS between days 21-29. αMyHC/CFA immunization resulted in myocarditis in *Nos2*$^{-/-}$ mice (not shown), but M-CSF treatment failed to affect fibrosis and heart functions during the post-inflammatory phase of EAM in *Nos2*$^{-/-}$ mice (Figure 6A, Supplementary figure 6). Similar results were observed if mice were M-CSF treated between days 14-22 (not shown). M-CSF treatment of *Nos2*$^{-/-}$ mice failed to increase the numbers of $F4/80^+$ macrophages and $CD133^+$ cells in the myocardium at day 24 and 40 of EAM (Figure 6A-C). We also observed no differences in F4/80 expression on inflammatory $CD133^+/CD45^+$ progenitors (not shown) and in the expression of M1/M2 markers on heart infiltrating $F4/80^+/CD45^+$ macrophages between M-CSF- and PBS-treated *Nos2*$^{-/-}$ mice (Figure 6D).

Discussion

We previously reported that in the EAM model post-inflammatory pathogenic myofibroblasts mainly originate from heart-infiltrating CD133$^+$ progenitor cells[6]. In line with our previous findings, herein we demonstrate that M-CSF controls the formation of anti-inflammatory macrophages from inflammatory CD133$^+$ progenitors and prevents TGF-β-mediated differentiation into pathogenic myofibroblasts. Thus, our data suggest that in myocarditis, a significant pool of cells infiltrating the myocardium at the peak of disease represent non-committed progenitors.

From a clinical perspective it is important that the differentiation fate of multipotent, non-committed precursor cells infiltrating the myocardium, can be modulated via specific cytokine signalling in a controlled fashion. M-CSF is a key cytokine guiding macrophage differentiation *in vitro*[8] and *in vivo*[18]. In EAM, M-CSF treatment up-regulated F4/80 expression on CD133$^+$ inflammatory progenitors promoting macrophage differentiation. In untreated mice, however, heart-infiltrating CD133$^+$ progenitors spontaneously differentiate into pathogenic myofibroblasts. To our knowledge, this is the first report describing the change of *in vivo* fate of inflammatory progenitors naturally present in the inflamed organ. So far, it has been described that M-CSF treatment improved cardiac function in a viral model of myocarditis[16], after myocardial infarction[14, 15, 19] and in the ischemia-reperfusion model[20]. Similar to our findings, M-CSF treatment promoted monocyte/macrophage accumulation in the heart after myocardial infarction[14, 15] or virus inoculation[16].

Myocardial fibrosis plays a dual role in remodelling after cardiac injury. On one hand, it is a prerequisite for wound healing, as in case of ischemic injuries, for example. On the other hand, it contributes to ventricular stiffening and typical pathological remodelling in heart failure. Our previous and current data clearly show that excessive cardiac fibrosis parallels impaired cardiac function in EAM[17]. Thus, preserved left ventricular function in M-CSF-treated mice results primarily from reduced myofibroblast differentiation, rather than protective macrophage activity. We propose that the conversion of inflammatory progenitors into functional macrophages, instead of myofibroblasts, represent a key mechanism explaining reduced fibrogenesis upon M-CSF treatment. However, we cannot rule out that M-CSF also activates other pathways inhibiting myocardial fibrogenesis. For example, M-CSF may protect cardiomyocytes from H_2O_2-induced death[20]. Moreover, M-CSF could affect extracellular matrix composition and levels of matrix

metalloproteinases and cytokines/chemokines, which drastically alter the myocardial microenvironment. Nevertheless, we can exclude direct M-CSF-mediated effects on cardiac fibroblasts, because upon M-CSF treatment during the late post-inflammatory phase of the EAM (days 40-48), the fibrosis was not reverted.

It has been proposed that differential macrophage activation defines protective and pathogenic functions. Accordingly, adoptive transfer of M1 macrophages promoted histological disease scores, whereas injection of M2 macrophages was largely protective in Coxackievirus-induced myocarditis[9]. Also most heart-infiltrating macrophages were classified as M2 macrophages expressing mannose receptor and Gr-1 in αMyHC/CFA- and Coxackievirus-induced myocarditis[7, 21]. However, macrophages expressing M1 marker NOS2 have been identified in myocarditis as well[22]. We critically analysed macrophages in the myocardium after the peak of disease, during the post-inflammatory phase of EAM, and detected both, M1- and M2-specific markers. We were, however, unable to clearly delineate two distinct activation states. We assume that during EAM, heart-infiltrating macrophages were activated classically (M1) and alternatively (M2) at the same time. In fact, it is well known that T cells and other heart-infiltrating cells massively produce both, M1-activating IFN-γ as well as M2-activating IL-4 and IL-13[7]. Importantly, M-CSF treatment did not affect the expression of M1 and M2 markers except of NOS2. M-CSF-induced macrophage accumulation in the post-inflammatory heart was not pathogenic in our model, because resolution of inflammation, defined by the extent of inflammatory cells was clearly M-CSF independent. Moreover, M-CSF-induced macrophages showed strong immunosuppressive activity *in vitro* and *in vivo*. We believe that accumulation of the immunosuppressive macrophages in M-CSF-treated mice protected from spontaneous T cell relapse. Nevertheless, we cannot, entirely rule out that M-CSF also mediates protective effects by acting on other target cells.

We previously found that M-CSF-induced $CD11b^+$ monocytes prevented EAM development and suppressed $CD4^+$ T cell proliferation in a nitric oxide-dependent manner[23]. M-CSF treatment promoted inflammatory macrophages expressing NOS2 in EAM, We therefore hypothesized that macrophage-produced nitric oxide might control both; T cell mediated early inflammation as well as post-inflammatory fibrosis in EAM. Indeed, mice lacking NOS2 or treated with nitric oxide inhibitors showed enhanced cardiac inflammation and fibrotic lesions in a model of Coxackievirus-induced myocarditis[24, 25]. Similarly, *Nos2*$^{-/-}$ mice also develop more severe myocarditis in the EAM model (*Kania, Blyszczuk & Eriksson- unpublished*

observations). Nevertheless, we observed spontaneous resolution of inflammation in *Nos2*$^{-/-}$ mice, suggesting that NOS2 is not critically involved in the resolution of inflammation in the EAM model. Surprisingly, treatment of *Nos2*$^{-/-}$ mice with M-CSF failed to turn CD133^{+} progenitors into macrophages and to prevent fibrosis development. Furthermore, we showed that *Nos2*$^{-/-}$ CD133^{+} progenitors stimulated with M-CSF failed to generate functional macrophages. These results suggested that NOS2 was required for M-CSF-induced macrophage differentiation and maturation. Accordingly, NOS2 has been reported to control differentiation of human monoblasts[26]. Regulation of gene expressions by nitric oxide can explain requirement of NOS2 in this differentiation processes[27]. At this stage, we cannot, however, exclude that in *Nos2*$^{-/-}$ mice, heart-infiltrating CD133^{+} progenitors are committed toward fibroblast phenotype due to alerted cytokine expression profile in the myocardium. Based on our findings, we can assume that M-CSF stimulates nitric oxide production that, in turn, promotes macrophage differentiation of inflammatory progenitors.

In summary, our data demonstrate that a single hematopoietic cytokine, such as M-CSF can modulate the *in vivo* fate of inflammatory CD133^{+} progenitors in a way to promote their differentiation into macrophages instead of myofibroblasts in the post-inflammatory phase of the EAM. Furthermore, our data suggest that mature inflammatory macrophages, in contrast to progenitor-derived fibroblasts, do not promote heart failure after acute myocarditis. These findings are in line with the clinical observation that fulminant myocarditis implies an excellent long-term prognosis whereas subacute myocarditis usually progresses to end stage heart failure[28].

Acknowledgment

We thank Marta Bachman for excellent technical assistance, Flow Cytometry Facility at University Zurich for excellent sorting service and Dr. Pavani Mocharla for critical reading.

Funding

U.E. acknowledges support from the Swiss Life Foundation, P.B. from the Swiss Heart Foundation and G.K. from the Olga Mayenfisch Foundation, Hartmann Müller Foundation, and Holcim Foundation. The study was supported by the Swiss National Science Foundation (U.E. and G.K.: Grant 32003B_130771) and Swiss

National Science Foundation MHV subsidy (G.K.: Grant PMPDP3_129013).

Conflict of Interest

None

References:

1. Aretz HT, Billingham ME, Edwards WD, Factor SM, Fallon JT, Fenoglio JJ, Jr. *et al.* Myocarditis. A histopathologic definition and classification. *Am J Cardiovasc Pathol.* 1987;**1**:3-14.

2. Kishimoto C, Abelmann WH. In vivo significance of T cells in the development of Coxsackievirus B3 myocarditis in mice. Immature but antigen-specific T cells aggravate cardiac injury. *Circ Res.* 1990;**67**:589-598.

3. Leuschner F, Katus HA, Kaya Z. Autoimmune myocarditis: past, present and future. *J Autoimmun.* 2009;**33**:282-289.

4. Rose NR. Myocarditis: infection versus autoimmunity. *J Clin Immunol.* 2009;**29**:730-737.

5. Kania G, Blyszczuk P, Eriksson U. Mechanisms of cardiac fibrosis in inflammatory heart disease. *Trends Cardiovasc Med.* 2009;**19**:247-252.

6. Kania G, Blyszczuk P, Stein S, Valaperti A, Germano D, Dirnhofer S *et al.* Heart-infiltrating prominin-1+/CD133+ progenitor cells represent the cellular source of transforming growth factor beta-mediated cardiac fibrosis in experimental autoimmune myocarditis. *Circ Res.* 2009;**105**:462-470.

7. Fairweather D, Cihakova D. Alternatively activated macrophages in infection and autoimmunity. *J Autoimmun.* 2009;**33**:222-230.

8. Gordon S, Martinez FO. Alternative activation of macrophages: mechanism and functions. *Immunity.* 2010;**32**:593-604.

9. Li K, Xu W, Guo Q, Jiang Z, Wang P, Yue Y *et al.* Differential macrophage polarization in male and female BALB/c mice infected with coxsackievirus B3 defines susceptibility to viral myocarditis. *Circ Res.* 2009;**105**:353-364.

10. Parissis J, Filippatos G, Adamopoulos S, Li X, Kremastinos DT, Uhal BD. Hematopoietic colony stimulating factors in cardiovascular and pulmonary remodeling: promoters or inhibitors? *Curr Pharm Des.* 2006;**12**:2689-2699.

11. Hamilton JA. Colony-stimulating factors in inflammation and autoimmunity. *Nat Rev Immunol.* 2008;**8**:533-544.

12. Wiktor-Jedrzejczak W, Gordon S. Cytokine regulation of the macrophage (M phi) system studied

using the colony stimulating factor-1-deficient op/op mouse. *Physiol Rev.* 1996;**76**:927-947.

13. Naito M, Hayashi S, Yoshida H, Nishikawa S, Shultz LD, Takahashi K. Abnormal differentiation of tissue macrophage populations in 'osteopetrosis' (op) mice defective in the production of macrophage colony-stimulating factor. *Am J Pathol.* 1991;**139**:657-667.

14. Yano T, Miura T, Whittaker P, Miki T, Sakamoto J, Nakamura Y *et al.* Macrophage colony-stimulating factor treatment after myocardial infarction attenuates left ventricular dysfunction by accelerating infarct repair. *J Am Coll Cardiol.* 2006;**47**:626-634.

15. Morimoto H, Takahashi M, Shiba Y, Izawa A, Ise H, Hongo M *et al.* Bone marrow-derived CXCR4+ cells mobilized by macrophage colony-stimulating factor participate in the reduction of infarct area and improvement of cardiac remodeling after myocardial infarction in mice. *Am J Pathol.* 2007;**171**:755-766.

16. Hiraoka Y, Kishimoto C, Takada H, Suzaki N, Shiraki K. Colony-stimulating factors and coxackievirus B3 myocarditis in mice: macrophage colony-stimulating factor suppresses acute myocarditis with increasing interferon-alpha. *Am Heart J.* 1995;**130**:1259-1264.

17. Blyszczuk P, Kania G, Dieterle T, Marty RR, Valaperti A, Berthonneche C *et al.* Myeloid differentiation factor-88/interleukin-1 signaling controls cardiac fibrosis and heart failure progression in inflammatory dilated cardiomyopathy. *Circ Res.* 2009;**105**:912-920.

18. Wiktor-Jedrzejczak W, Ratajczak MZ, Ptasznik A, Sell KW, Ahmed-Ansari A, Ostertag W. CSF-1 deficiency in the op/op mouse has differential effects on macrophage populations and differentiation stages. *Exp Hematol.* 1992;**20**:1004-1010.

19. Miki T, Miura T, Nishino Y, Yano T, Sakamoto J, Nakamura Y *et al.* Granulocyte colony stimulating factor/macrophage colony stimulating factor improves postinfarct ventricular function by suppression of border zone remodelling in rats. *Clin Exp Pharmacol Physiol.* 2004;**31**:873-882.

20. Okazaki T, Ebihara S, Asada M, Yamanda S, Saijo Y, Shiraishi Y *et al.* Macrophage colony-stimulating factor improves cardiac function after ischemic injury by inducing vascular endothelial growth factor production and survival of cardiomyocytes. *Am J Pathol.* 2007;**171**:1093-1103.

21. Cihakova D, Barin JG, Afanasyeva M, Kimura M, Fairweather D, Berg M *et al.* Interleukin-13 protects against experimental autoimmune myocarditis by regulating macrophage differentiation.

Am J Pathol. 2008;**172**:1195-1208.

22. Lowenstein CJ, Hill SL, Lafond-Walker A, Wu J, Allen G, Landavere M *et al.* Nitric oxide inhibits viral replication in murine myocarditis. *J Clin Invest.* 1996;**97**:1837-1843.

23. Valaperti A, Marty RR, Kania G, Germano D, Mauermann N, Dirnhofer S *et al.* CD11b+ monocytes abrogate Th17 CD4+ T cell-mediated experimental autoimmune myocarditis. *J Immunol.* 2008;**180**:2686-2695.

24. Zaragoza C, Ocampo C, Saura M, Leppo M, Wei XQ, Quick R *et al.* The role of inducible nitric oxide synthase in the host response to Coxsackievirus myocarditis. *Proc Natl Acad Sci U S A.* 1998;**95**:2469-2474.

25. Hiraoka Y, Kishimoto C, Takada H, Nakamura M, Kurokawa M, Ochiai H *et al.* Nitric oxide and murine coxsackievirus B3 myocarditis: aggravation of myocarditis by inhibition of nitric oxide synthase. *J Am Coll Cardiol.* 1996;**28**:1610-1615.

26. Kim SJ, Bang OS, Lee YS, Kang SS. Production of inducible nitric oxide is required for monocytic differentiation of U937 cells induced by vitamin E-succinate. *J Cell Sci.* 1998;**111 (Pt 4)**:435-441.

27. Wink DA, Hines HB, Cheng RY, Switzer CH, Flores-Santana W, Vitek MP *et al.* Nitric oxide and redox mechanisms in the immune response. *J Leukoc Biol.* 2011;**89**:873-891.

28. McCarthy RE, 3rd, Boehmer JP, Hruban RH, Hutchins GM, Kasper EK, Hare JM *et al.* Long-term outcome of fulminant myocarditis as compared with acute (nonfulminant) myocarditis. *N Engl J Med.* 2000;**342**:690-695.

Figure legends

Figure 1. M-CSF prevents differentiation of heart-infiltrating CD133$^+$ progenitors into myofibroblasts.

(A,B) Heart-infiltrating CD133$^+$ cells were expanded from myocarditis-positive hearts at day 21 of EAM and stimulated without (control, white) or with 10 ng/mL M-CSF (gray), or 10 ng/mL TGF-β (black) for 14 days. Relative mRNA expression of myofibroblast-specific fibronectin (*Fn1*), collagen I (*Col1a1*) and αSMA (*Acta2*) (A, n=5). Representative immunofluorescence and quantification analysis of αSMA (top) and fibronectin (bottom) in cultured cells (B, n=5).

(C,D) Expanded heart-infiltrating CD133$^+$ cells (EAM d21) pre-treated for 3 days without (control, black) or with 10 ng/mL M-CSF (+M-CSF d-3, hatch), washed and stimulated with 10 ng/mL TGF-β for 14 days. Relative mRNA levels of myofibroblast-specific genes (C, n=5) and representative immunofluorescence and quantification analysis of αSMA (D, top) and fibronectin (D, bottom) are shown (n=5).

*** p<0.001 (two-tailed Student's *t*-test versus control), bar = 20μm.

Figure 2. M-CSF treatment turns inflammatory CD133$^+$ progenitors into F4/80$^+$ macrophages in EAM.

BALB/c mice were immunized with αMyHC/CFA at day 0 and 7, and treated with PBS or M-CSF between days 21-29.

(A) Quantification of F4/80$^+$ macrophages in the myocardium of PBS- (black) and M-CSF-treated (white) mice at day 24 (n=6), 28 (n=5) and 40 (n=20). Immunopositive cells were quantified per mm^2 of heart tissue.

(B) Flow cytometry analysis of CD133 and F4/80 on heart infiltrating CD45$^+$-gated cells (left) in EAM. Quantification of CD133$^+$ (left graph) and F4/80$^+$ (right graph) cells gated on CD45$^+$ infiltrates of PBS- (black) and M-CSF-treated (white) mice at day 24 (n=5) and 28 (n=5) of EAM.

(C-G) Flow cytometry analysis of M1 and M2 activation markers on heart infiltrating CD45$^+$/F4/80$^+$-gated macrophages (left) in EAM. Mean fluorescence intensity (MFI) of membrane markers (CD16/32, CD206, CD301) and intracellular NOS2 expression gated on inflammatory macrophages of PBS- (black) and M-CSF-treated (white) mice at day 24 (n=10) of EAM. (–) isotype controls, (+) antigen-specific antibodies.

(H) Overlay of phase contrast (left and middle) or F4/80 expression (right, red) with *E.coli* bacteria (green) taken up in the phagocytosis assay of expanded heart-infiltrating $CD133^+$ cells (isolated from heart at d21) stimulated with M-CSF for 1 (left) and 3 days (middle and right). Bar = 20µm.

ns $p>0.05$, * $p<0.05$, ** $p<0.01$, *** $p<0.001$ (two-tailed Student's *t*-test).

Figure 3. M-CSF inhibits myofibroblast lineage differentiation of inflammatory $CD133^+$ in EAM.

(A) Representative flow cytometry analysis of $CD133^+$ and F4/80 (right) gated on heart infiltrating $CD45^+$ cells (left) at day 24 of EAM. Numbers indicate percentage of positive cells in the adjacent gates.

(B) Heart-infiltrating $CD45^+/CD133^+/F4/80^-$ (white) and $CD45^+/CD133^+/F4/80^{hi}$ (black) cells were FACS sorted from myocarditis-positive hearts at day 24 of EAM. Relative mRNA levels of myofibroblast-specific genes are shown for 1 out of 2 independent experiments (n=5).

(C) Representative flow cytometry analysis of CD133 and F4/80 gated on heart infiltrating $CD45^+/CD133^+$ progenitor cells (left) of PBS- (+PBS) and M-CSF-treated (+M-CSF) mice at day 24 of EAM. Staining with anti-CD45 and anit-CD133 and IgG control to anti-F4/80 antibodies (IgG control) was used to set the gates. Numbers indicate percentage of positive cells in the adjacent gates.

(D) Quantification of $F4/80^{hi}$ (left) and $F4/80^-$ (right) cells gated of $CD45^+/CD133^+$ progenitor cells (gated as shown in C) of PBS- (black) and M-CSF-treated (white) mice at day 24 of EAM.

(E,F) Heart-infiltrating $CD45^+/CD133^+$ cells were FACSorted from myocarditis-positive hearts at day 24 of EAM from control PBS-treated (black, +PBS) or M-CSF-treated (white, +M-CSF). A relative mRNA level of myofibroblast-specific genes of sorted cells is shown (E, n=5). In addition, sorted cells were plated and stimulated with 10 ng/mL TGF-β for 10 days. Representative immunofluorescence and quantification analysis of αSMA (F, top) and fibronectin (F, bottom) are shown (n=5).

Bar = 20µm, ns $p>0.05$, * $p<0.05$, ** $p<0.01$, *** $p<0.001$ (two-tailed Student's *t*-test).

Figure 4. NOS2 is required for M-CSF-dependent macrophage lineage differentiation from $CD133^+$ progenitors.

(A-E) Expanded heart-infiltrating $CD133^+$ cells (EAM d21) from wild-type BALB/c and $Nos2^{-/-}$ mice were stimulated with 10 ng/mL M-CSF for 3 days. (A) Representative flow cytometry analysis of expanded cells

using anti-CD133 (right) and IgG control (left) antibodies. Numbers indicate percentage of positive cells in the adjacent gates. Representative histogram analysis of macrophage specific antigens F4/80 (B), CD11b (C), CD14 (D), and *E.coli* bacteria taken up in the phagocytosis assay (E) on $CD133^+$ cells (gated as shown in A). Isotype controls are displayed in grey. Numbers in histograms indicate mean fluorescence intensity (MFI). Bar graphs show quantification of the respective analyses for wild-type (black) and $Nos2^{-/-}$ (hatch) cells. n=5, (–) isotype controls, (+) antigen-specific antibodies or *E.coli*.

(F) Expanded heart-infiltrating $CD133^+$ cells (EAM d21) from BALB/c (wild-type) mice were stimulated with 10 ng/mL M-CSF for 3 days in the absence (control) or presence of 2mM L-NAME (+L-NAME). Representative histogram analysis of *E.coli* bacteria uptake by $CD133^+$ cells (gated as shown in A). Controls without *E.coli* are displayed in grey. Numbers in histograms indicate MFI. Bar graphs show quantification of the respective analyses in the absence (white) or presence of L-NAME (grey). n=5, (–) control, (+) *E.coli*

(G) Nitrite levels in supernatants of cultures stimulated with 0.1 µg/mL LPS for 24h. n = 4

ns $p>0.05$, * $p<0.05$, ** $p<0.01$, *** $p<0.001$ (two-tailed Student's *t*-test).

Figure 5. M-CSF treatment attenuates myocardial fibrosis and prevents heart failure in EAM.

BALB/c mice were immunized at day 0 and 7 with αMyHC/CFA and injected either with PBS (black) or M-CSF between days 21-29 (white) or days 40-48 (grey).

(A) Fibrosis was evaluated in heart sections at day 24 (n=10), 28 (n=10), 40 (n=20) and 60 (n=6-8). The degree of fibrosis was analysed by Masson's trichrome staining and calculated as percentage of the fibrotic area in heart sections.

(B,C) The representative microphotographs of the myocardial tissue (d60) following PBS (B) or M-CSF (C) treatment between days 21-29 stained with Masson's trichrome. Bar = 100 µm.

p values were computed using two-tailed Student's t-test (A, d24, d28 and d40), one-way ANOVA (A, d60).

(D-E) Quantification of $CD45^+$ cells (defining all inflammatory infiltrates, D) and $CD3^+$ cells (defining T lymphocytes, E) within the myocardium during EAM at day 24 (n=10), 28 (n=10), 40 (n=20) and 60 (n=6-8) after the first immunization. Immunopositive cells were quantified per mm^2 of heart tissue.

(F) Echocardiographic parameters of healthy, untreated BALB/c mice (white) in comparison to

αMyHC/CFA-immunised mice with <2% myocardial fibrosis (hatch, n=9), >2% myocardial fibrosis (black, n=11) and αMyHC/CFA-immunised mice treated with M-CSF at days 21-29 (grey, n=20).

p values were computed using correlation analysis (F) and the one-way ANOVA (A,D,E). * $p<0.05$, ** $p<0.01$, *** $p<0.001$ for the respective group versus healthy controls (white) calculated with Bonferroni post-hoc test.

Figure 6. M-CSF treatment fails to reduce fibrosis in *Nos2*$^{-/-}$ mice.

Nos2$^{-/-}$ mice were immunized at day 0 and 7 with αMyHC/CFA and treated with PBS or M-CSF between days 21-29.

(A,B) Quantification of fibrosis and F4/80^{+} macrophages in the myocardium of PBS- (black) and M-CSF-treated (white) *Nos2*$^{-/-}$ mice at day 24 (A, n=5) and 40 (B, n=10) of EAM. F4/80^{+} cells were quantified per mm^{2} of heart tissue, and the degree of fibrosis was analysed by Masson's trichrome staining.

(C) Representative histograms of CD133 expression gated on heart infiltrating CD45^{+} inflammatory cells (left) of PBS- (+PBS) and M-CSF-treated (+M-CSF) *Nos2*$^{-/-}$ mice at day 24 of EAM. Isotype controls are displayed in grey. Numbers indicate percentage of positive cells in the presented histograms. Bar graphs show quantification of CD133^{+} and F4/80^{+} gated on CD45^{+} cells of PBS- (black) and M-CSF-treated (white) *Nos2*$^{-/-}$ mice (n=5).

(D) Flow cytometry analysis of M1 and M2 activation markers in EAM. Quantification of mean fluorescence intensity (MFI) of membrane macrophage activation markers gated on heart infiltrating CD45^{+}/F4/80^{+}-gated macrophages (left) of PBS- (grey) and M-CSF-treated (hatch) *Nos2*$^{-/-}$ mice at day 24 of EAM (n=5). (–) isotype controls, (+) antigen-specific antibodies, ns $p>0.05$ (two-tailed Student's *t*-test).

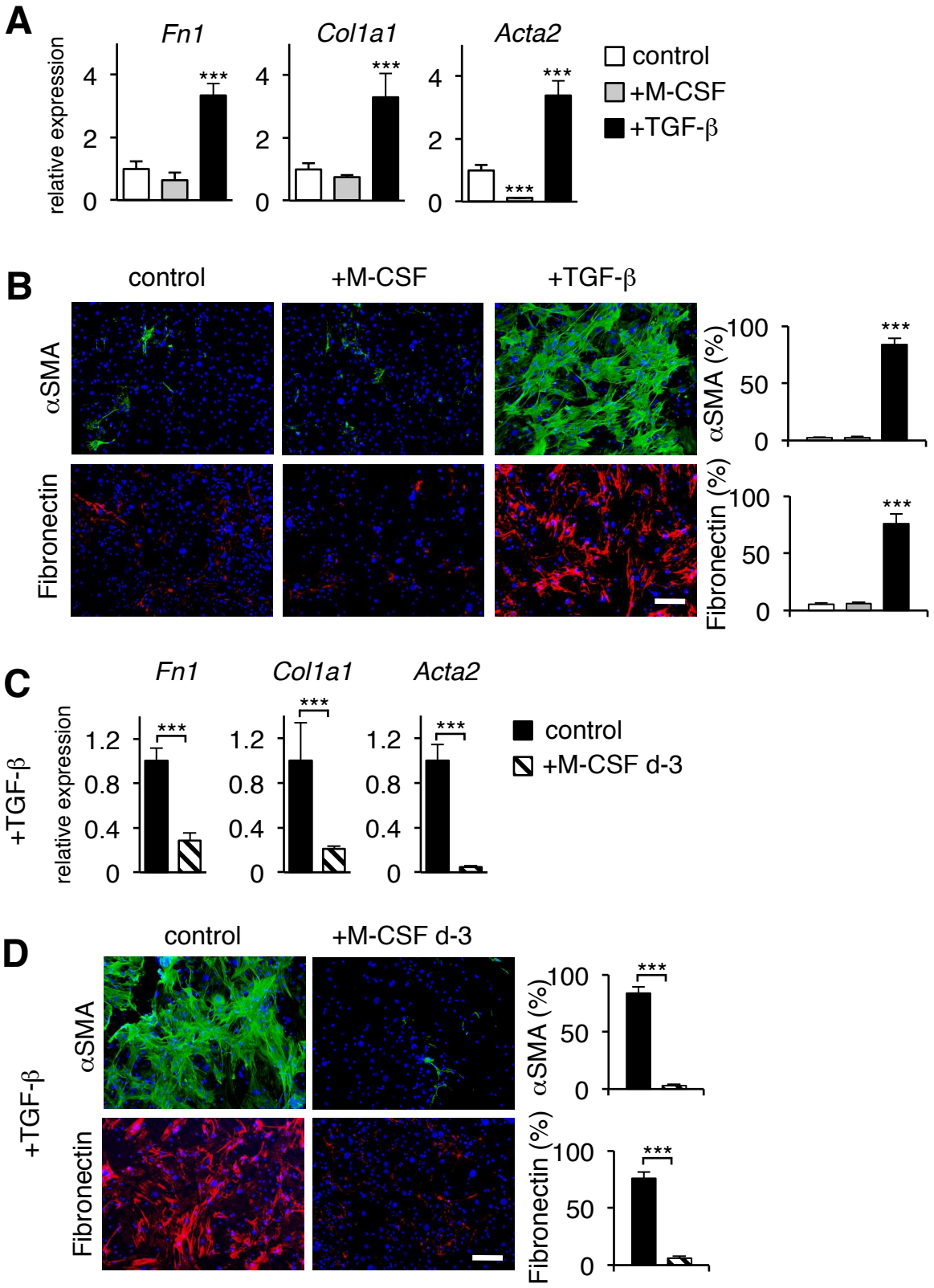

Blyszczuk et al., Figure 1

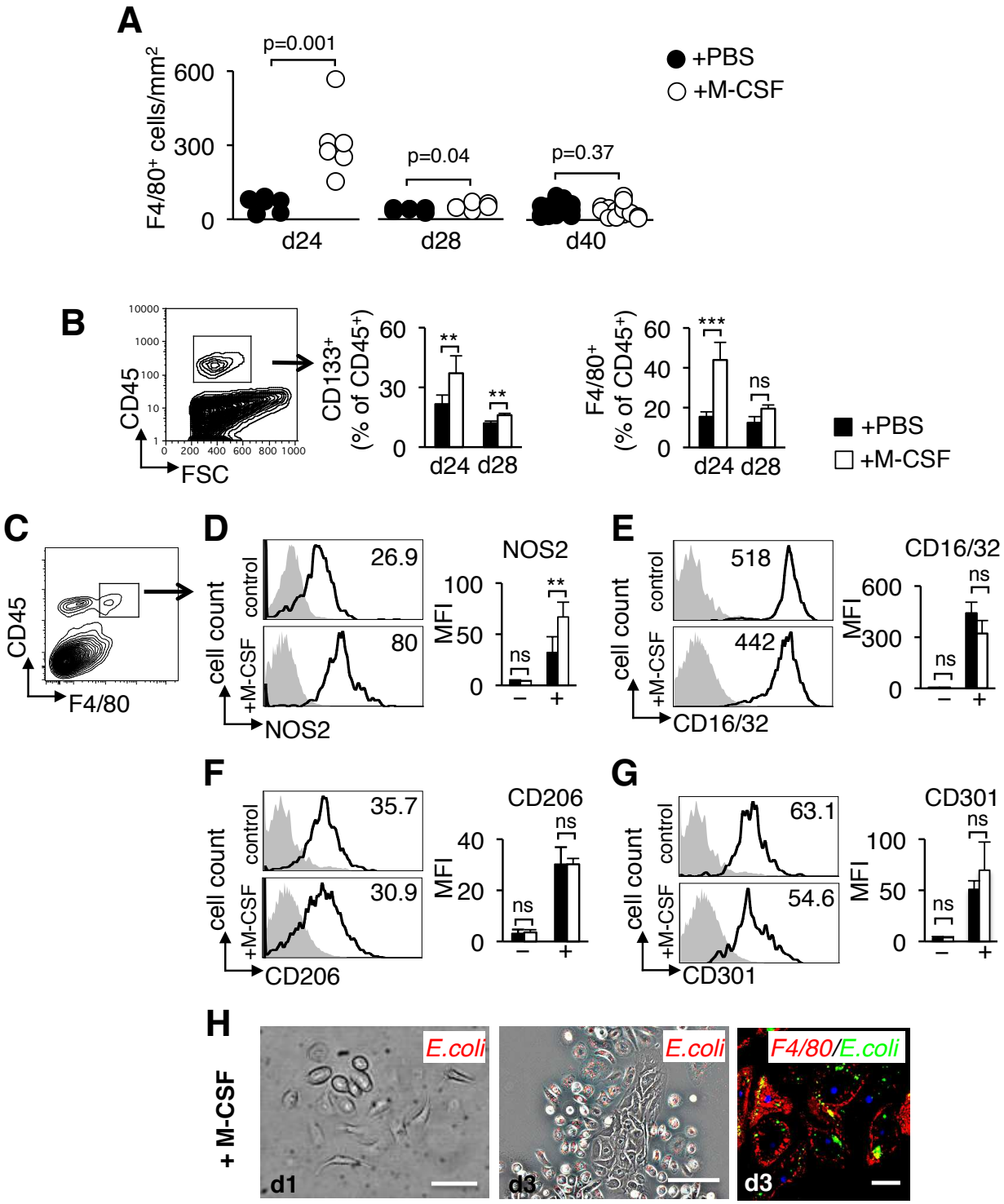

Blyszczuk et al., Figure 2

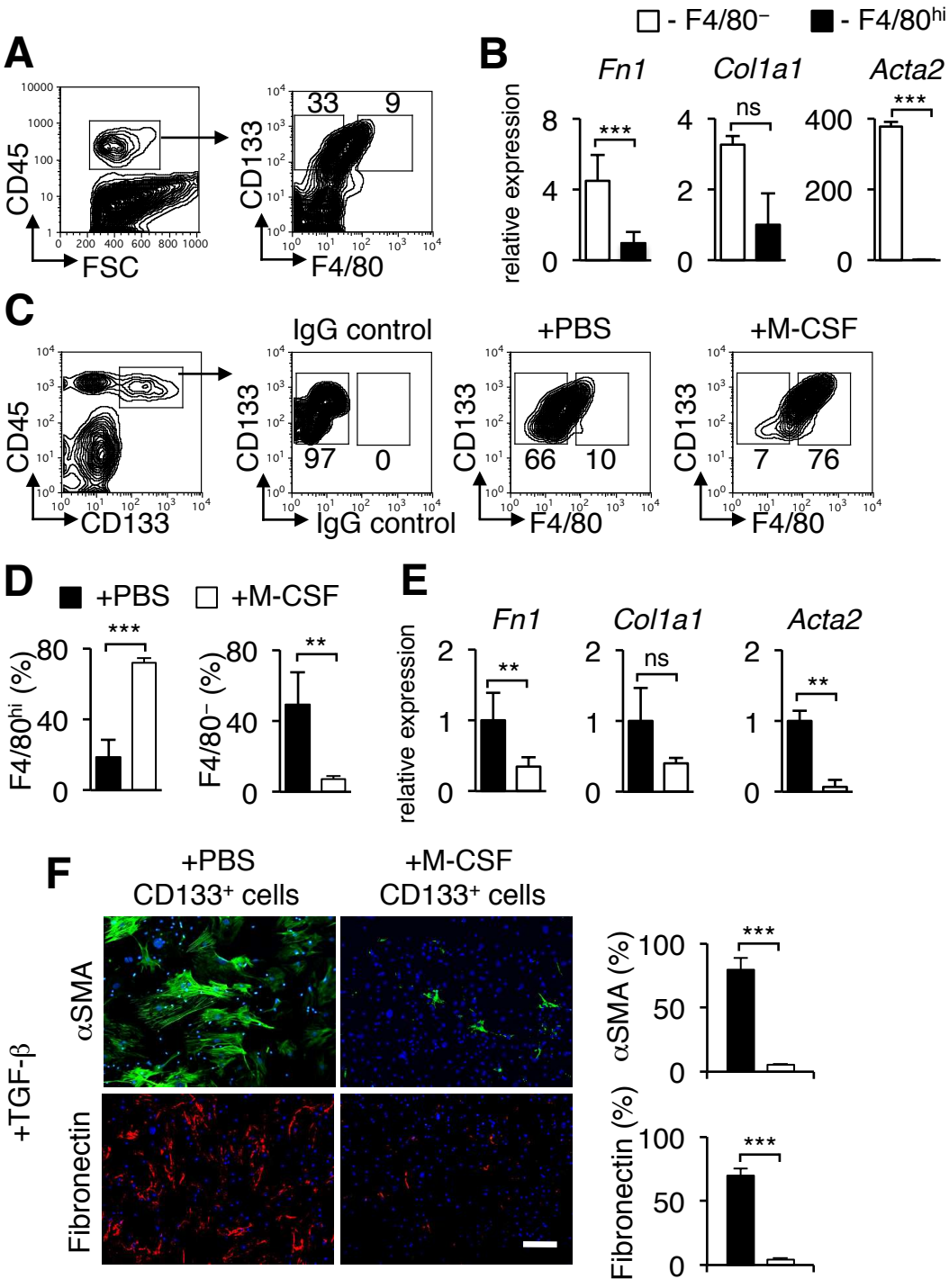

Blyszczuk et al., Figure 3

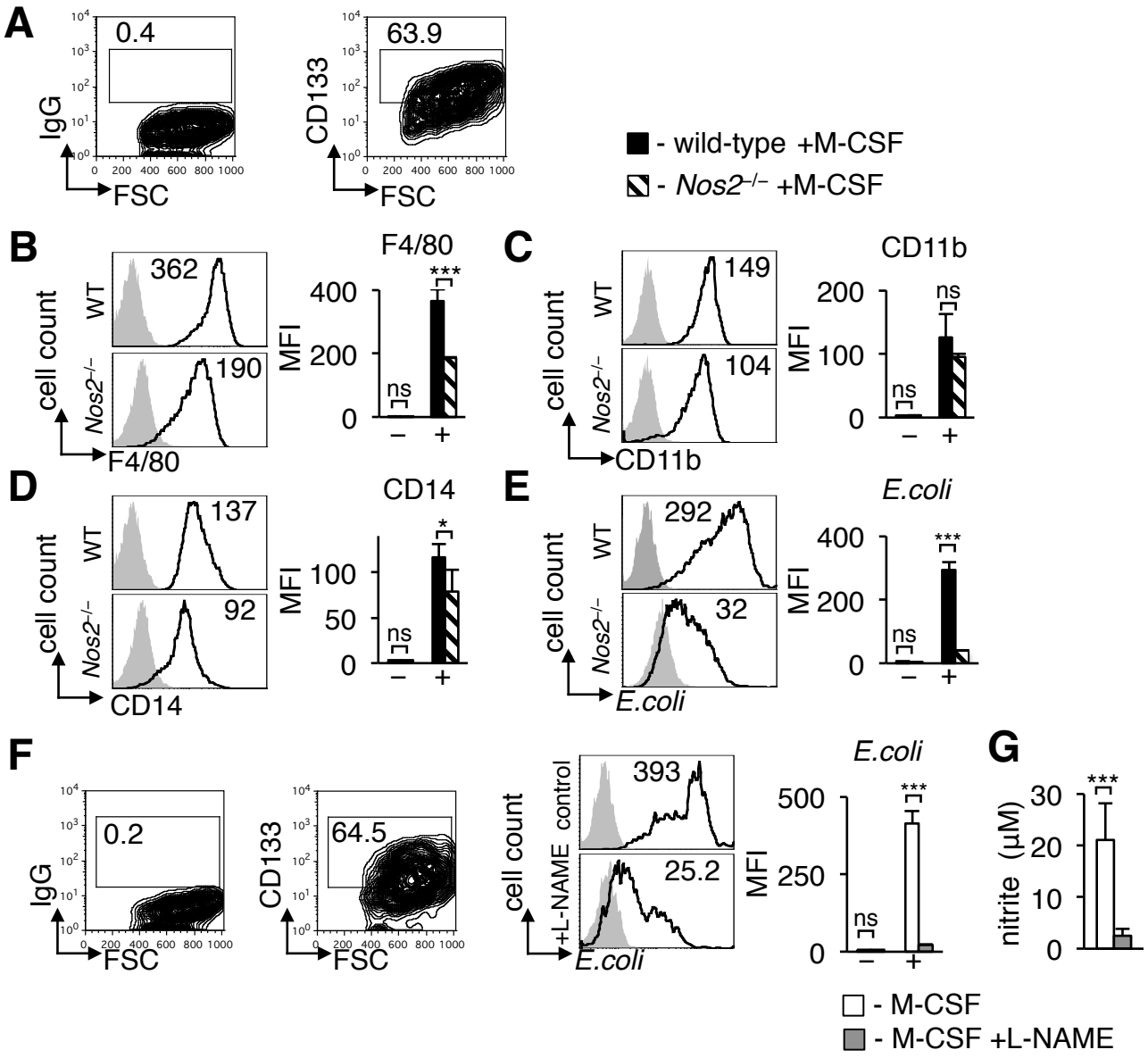

Blyszczuk et al., Figure 4

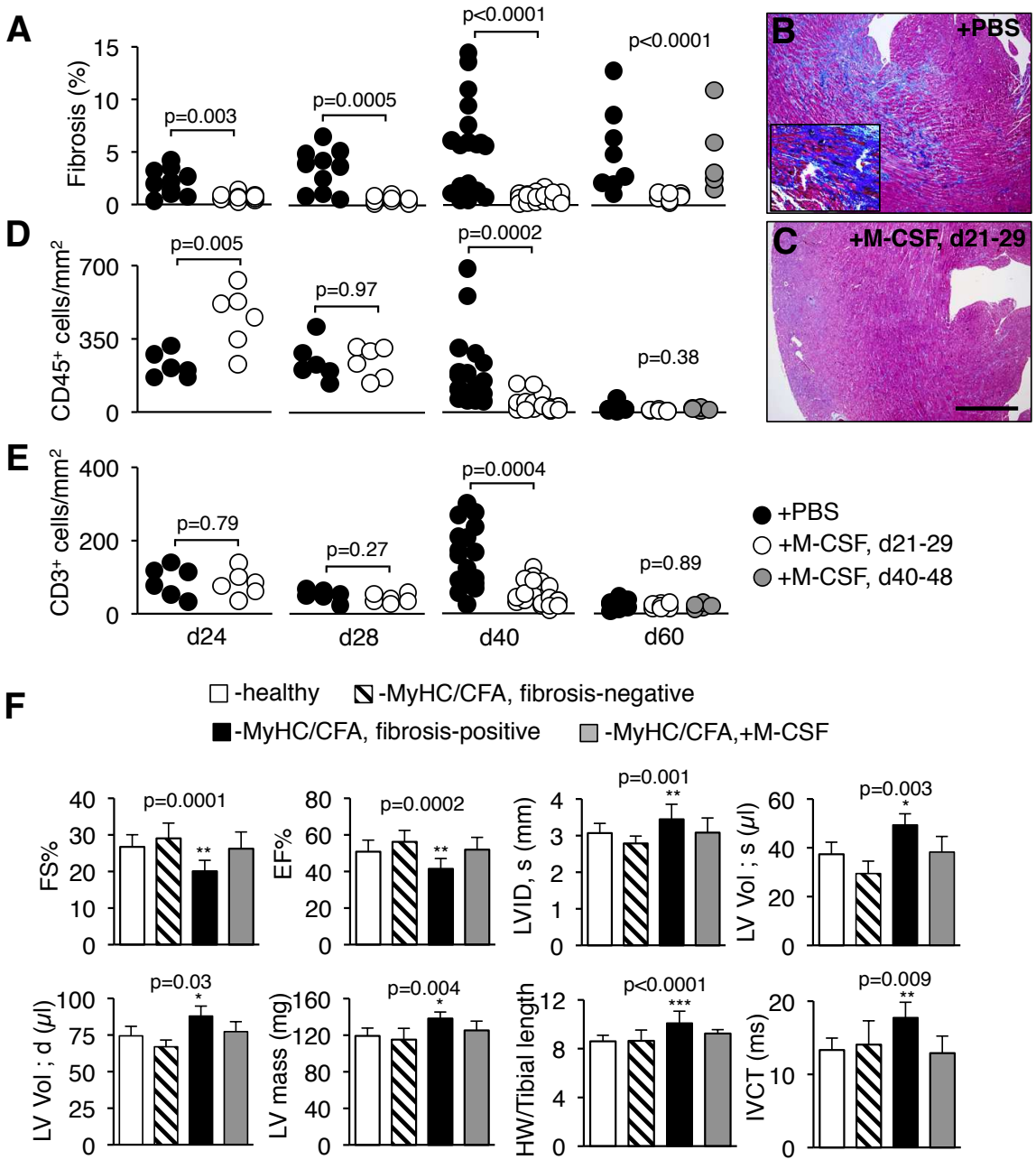

Blyszczuk et al., Figure 5

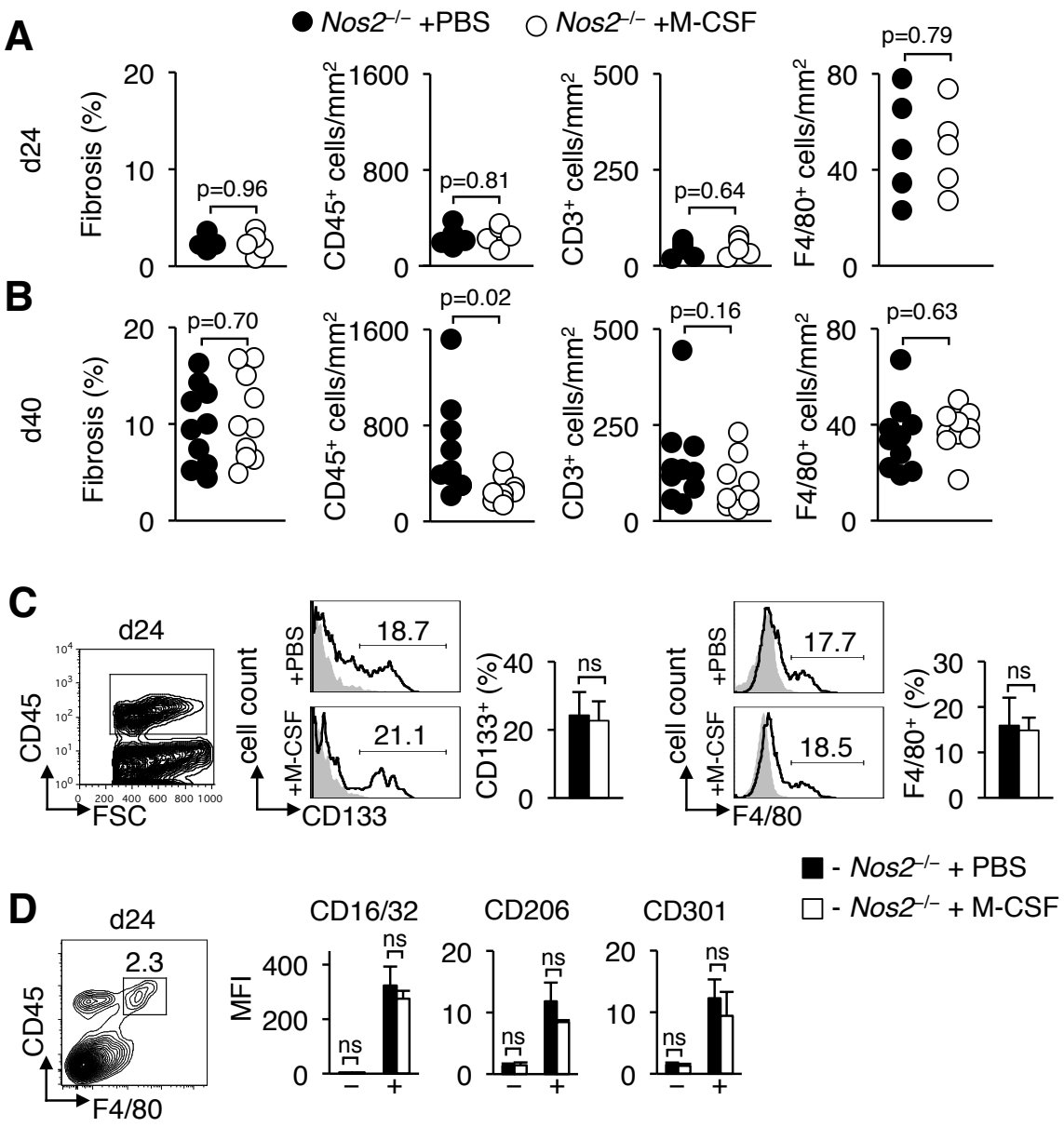

Blyszczuk et al., Figure 6